



Published in final edited form as:

*J Am Chem Soc.* 2013 July 3; 135(26): 9560–9563. doi:10.1021/ja4001129.

## A $^{13}\text{C}$ labeling strategy reveals a range of aromatic side chain motion in calmodulin

Vignesh Kasinath, Kathleen G. Valentine, and A. Joshua Wand

Graduate Group in Biochemistry and Molecular Biophysics and the Johnson Research Foundation and Department of Biochemistry and Biophysics, University of Pennsylvania Perelman School of Medicine, Philadelphia 19104, United States of America

### Abstract

NMR relaxation experiments often require site-specific isotopic enrichment schemes in order to allow for quantitative interpretation. Here, we describe a new labeling scheme for site-specific  $^{13}\text{C}$ - $^1\text{H}$  enrichment of a single ortho position of aromatic amino acid side chains in an otherwise perdeuterated background by employing a combination of [4- $^{13}\text{C}$ ]-erythrose and deuterated pyruvate during growth on deuterium oxide. This labeling scheme largely eliminates undesired contributions to  $^{13}\text{C}$  relaxation and greatly simplifies the fitting of relaxation data using Lipari-Szabo model-free formalism. This approach is illustrated with calcium-saturated vertebrate calmodulin and oxidized flavodoxin from *Cyanobacterium anabaena*. Analysis of  $^{13}\text{C}$ -relaxation aromatic groups of calcium-saturated calmodulin indicates a wide range of motion in the sub-nanosecond time regime.

Nuclear magnetic resonance (NMR) relaxation has proven to be a versatile probe of the link between fast internal protein motions and their relevance to function.<sup>1-4</sup> The motions of the polypeptide chain or of the amino acid side chains in proteins of significant size are most often studied using  $^{15}\text{N}$ -relaxation of amide nitrogen and deuterium or carbon relaxation in methyl groups.<sup>2,3</sup> This is generally due to restrictions arising from requirements of isotopic labeling and unfavorable relaxation properties of some sites within proteins. In other contexts, more specific and tailored enrichment schemes are often vital in order to eliminate unwanted dipolar and scalar interactions as well as to simplify data interpretation. Examples include use of [3- $^{13}\text{C}$ ]-pyruvate<sup>5</sup>, [2- $^{13}\text{C}$ ]-glycerol or [1,3- $^{13}\text{C}$ ]-glycerol<sup>6,7</sup> or mixtures of singly  $^{13}\text{C}$ -enriched acetates<sup>8</sup> as carbon precursors to generate isolated  $^{13}\text{C}$  spins. Even more selective spin enrichment schemes are sometimes required to suppress unwanted spin interactions and often employ more complex biosynthetic precursors. Prominent examples include labeling schemes targeted for optimal relaxation in methyl groups.<sup>5,9,10</sup> Comprehensive chemical synthesis, though relatively expensive, has also proven viable.<sup>11</sup>

Here we focus on the use of NMR relaxation phenomena to characterize the fast sub-nanosecond motion of aromatic residues. Aromatic amino acid side chains have a rich structural role within proteins<sup>12-15</sup> and are often central to their biological function particularly in the context of molecular recognition<sup>16,17</sup> and catalysis.<sup>18</sup> Thus the motional character of aromatic residues would seem to be of central importance in a range of protein structure-function issues. In this context, NMR phenomena have long been used to

Corresponding Author wand@mail.med.upenn.edu.

**Supporting Information.** Description of [4- $^{13}\text{C}$ ]-erythrose labeling protocol. Carbon-13 relaxation decay rates for aromatic side chains in calcium-saturated calmodulin collected at 500 MHz, 600 MHz and 750 MHz ( $^1\text{H}$ ).  $^{13}\text{C}$ -HSQC spectrum of flavodoxin prepared with the [4- $^{13}\text{C}$ ]-erythrose labeling strategy. This material is available free of charge via the Internet at <http://pubs.acs.org>.

characterize relatively slow motions that are manifested in line broadening or population exchange.<sup>19</sup>

For classical relaxation phenomena used to probe fast sub-nanosecond motions, aromatic residues present a difficult situation. In addition to the concern about the isolation of the spin interaction of interest from extraneous contributions, aromatic ring systems suffer from extensive homo- and heteronuclear scalar (J) interactions that can also significantly complicate the quality and information content of obtained relaxation data. Previously, 1-<sup>13</sup>C- or 2-<sup>13</sup>C-glucose has been used to create isolated <sup>13</sup>C sites in aromatic side chains and thereby eliminate one-bond <sup>13</sup>C-<sup>13</sup>C interactions. However, this labeling scheme does not eliminate remote scalar or dipolar interactions with non-bonded <sup>1</sup>H spins.<sup>20-22</sup> In our hands, the 1-<sup>13</sup>C glucose labeling scheme, which is designed to place isolated <sup>13</sup>C at the  $\delta$  position, results in minor scrambling of label that confounds somewhat the subsequent analysis (see below). In addition, though anticipated to be less of an issue than for methyl <sup>13</sup>C relaxation studies,<sup>9,23</sup> the presence of remote <sup>1</sup>H spins does present a complication to the analysis of aromatic <sup>13</sup>C relaxation in proteins. Isolation of the <sup>1</sup>H-<sup>13</sup>C pair in an otherwise perdeuterated background would eliminate potential complications from dipolar interactions with remote <sup>1</sup>H spins as well as scalar couplings with other ring hydrogens. Labeling strategies based on glucose are unable to provide this labeling scheme. To largely overcome this limitation we have developed a biosynthetic strategy that takes advantage of the flow of carbon from erythrose 4-phosphate (E4P) to the biosynthesis of the Tyr, Phe and Trp through condensation with phosphoenolpyruvate<sup>24</sup> (Figure 1). Consideration of this pathway suggests that use of [4-<sup>13</sup>C]-erythrose as a sole source of <sup>13</sup>C in conjunction with deuterated <sup>12</sup>C-pyruvate will lead to creation of an isolated bonded <sup>1</sup>H-<sup>13</sup>C pair at a *single* delta position (C2 position) within the aromatic ring. Protein expression during growth on [4-<sup>13</sup>C]-erythrose and deuterated <sup>12</sup>C-pyruvate and 99% D<sub>2</sub>O allows for exchange of all other non-aromatic hydrogens while preserving that bonded to the target <sup>13</sup>C. In the case of phenylalanine and tryptophan, an additional <sup>1</sup>H spin is predicted to remain at the  $\zeta$  position (C4 position) of the benzoid ring. Fortunately, this spin is greater than 3 Å away from the sole <sup>13</sup>C nucleus rendering its contribution to relaxation negligible. All other aromatic carbons remain NMR inactive <sup>12</sup>C nuclei. This labeling pattern therefore largely eliminates the potential complications of extraneous intra-ring scalar or dipolar interactions (<sup>1</sup>H or <sup>13</sup>C) with the isolated <sup>13</sup>C spin. The low gyromagnetic ratio of the replacement deuterons will cause them to contribute insignificantly to relaxation of the isolated <sup>13</sup>C nucleus. Similarly, the presence of random <sup>13</sup>C at natural abundance will also have negligible contribution to the measured relaxation of the target <sup>13</sup>C nucleus.

Vertebrate calmodulin was expressed in *E. coli*<sup>25</sup> to test this strategy. <sup>12</sup>C,<sup>2</sup>H-pyruvate was used to suppress scrambling of <sup>13</sup>C to other amino acids and to aid in perdeuteration of the aromatic ring. One-dimensional <sup>13</sup>C-filtered and unfiltered <sup>1</sup>H spectra reveal essentially complete deuteration of the protein except at single delta-positions in Tyr and Phe residues and the  $\zeta$  position (C4) of Phe (Figure 2). No protonation at the  $\epsilon$ -position (C3, C5) of the aromatic ring is observed. <sup>13</sup>C-labeling is restricted to the delta positions of Tyr and Phe. The enrichment of <sup>13</sup>C-<sup>1</sup>H pairs at the delta position was determined by comparison of the unfiltered <sup>1</sup>H spectrum and the <sup>13</sup>C-filtered <sup>1</sup>H spectrum with and without <sup>13</sup>C decoupling, and was found to be uniformly 67% (Supplementary Fig. S1). Analysis of the one-dimensional <sup>13</sup>C spectra with and without <sup>1</sup>H coupling confirmed that the isolated <sup>13</sup>C $\delta$ -<sup>1</sup>H has not been diluted with <sup>2</sup>H from solvent (Supplementary Fig. S3). The under-labeling of <sup>13</sup>C is a consequence of using a ratio of 3:2 for <sup>12</sup>C,<sup>2</sup>H-pyruvate to [4-<sup>13</sup>C]-erythrose, which is motivated by the need to suppress scrambling of <sup>13</sup>C to other amino acids or other positions in aromatic rings. This is a reasonable price to pay to maintain the fidelity of the <sup>13</sup>C nucleus for relaxation studies.

Calmodulin does not contain tryptophan. To confirm that appropriate labeling of Trp is also achieved, flavodoxin C55A was similarly prepared.<sup>26</sup> Flavodoxin has four Trp, eight Tyr, eight Phe and one His residue. The 22 anticipated aromatic <sup>1</sup>H-<sup>13</sup>C correlations are seen in the <sup>13</sup>C-HSQC spectrum (Supplementary Figure S4). No other significant <sup>13</sup>C-labeling was observed. Thus the desired labeling pattern was observed for all four aromatic amino acid side chains in the context of a perdeuterated background.

<sup>13</sup>C R<sub>1</sub> and R<sub>1ρ</sub> relaxation in calcium-saturated calmodulin prepared using this labeling strategy was measured at three magnetic fields (11.7, 14.0 and 17.6 T) using standard two-dimensional sampling pulse sequences.<sup>10</sup> For comparison, similar measurements were done using calmodulin prepared with a labeling strategy based on [1-<sup>13</sup>C]-glucose<sup>27,28</sup> (Figure 3). The anisotropy of global macromolecular tumbling was characterized in the usual way<sup>29</sup> using the crystal structure of calcium-saturated calmodulin (pdb code: 3CLN) and assessing the two globular domains separately.<sup>30</sup>

Lipari-Szabo model-free squared generalized order parameters ( $O^2$ ) and effective correlation times ( $\tau_c$ ) were determined using a grid search approach<sup>35</sup> and employed an effective bond length of 1.09 Å and residue-type specific chemical shift anisotropy tensors<sup>32</sup> with axially symmetric and anisotropic<sup>36</sup> CSA values for Phe and Tyr, respectively. The analysis was carried out with an updated version (Relxn2A) of our in-house software.<sup>23,35</sup> Standard statistical F-tests were used to determine if R<sub>ex</sub> terms were justified. None were found. The contributions from <sup>13</sup>C-<sup>2</sup>H remote dipolar coupling and <sup>13</sup>C-<sup>13</sup>C dipolar interaction due to natural abundance <sup>13</sup>C amounted to less than 0.05% of <sup>13</sup>C-<sup>1</sup>H direct bond dipolar interaction. Relaxation data obtained from the [4-<sup>13</sup>C]-erythrose labeling scheme sample fit well to the simple model-free spectra density (Table 1). Obtained squared generalized order parameters ranged from 0.47 to 0.96 indicating a rich spectrum of aromatic ring motion within calcium-saturated calmodulin on the sub-nanosecond time scale.

In contrast, though the primary R<sub>1</sub> and R<sub>1ρ</sub> relaxation time profiles derived from the calcium-saturated calmodulin obtained from the [1-<sup>13</sup>C]-glucose labeling scheme fitted reasonably to a single exponential decays (Figure 3), the obtained relaxation rates largely gave relatively poor fits to the L-S model-free interpretation (5-10% versus <1% residual error) (Supplementary Table S3). Inclusion of remote <sup>1</sup>H spin dipolar interaction as well as dipolar interaction with <sup>13</sup>Cε failed to recover the excellent statistics of the relaxation data derived from the more optimal [4-<sup>13</sup>C]-erythrose labeling scheme (Supplementary Fig. S5, Table. S3). It seems likely that unaccounted dipolar relaxation, intra-ring 1-bond <sup>13</sup>C-<sup>13</sup>C J-coupling, intra-ring 2-bond <sup>13</sup>Cδ-<sup>1</sup>Hε J-coupling effects contaminate the measurement and interpretation of <sup>13</sup>C-relaxation in structured proteins in a protonated background. This is consistent with the presence of additional peaks in the <sup>13</sup>C-<sup>1</sup>H HSQC spectrum of calmodulin derived from the [1-<sup>13</sup>C]-glucose labeling scheme (Supplementary Fig. S6). These additional peaks arise from partial <sup>13</sup>C labeling (~8 - 15%) at the Cε of the aromatic ring and are a consequence of the scrambling of <sup>13</sup>C label when using glucose as the carbon precursor. These considerations provide a plausible scenario where the relaxation profiles still fit reasonably to single exponential decays but fail to be fit reasonably by the L-S model-free formalism. Thus the [4-<sup>13</sup>C]-erythrose labeling strategy described here would seem to be highly advantageous in providing high fidelity relaxation for the study of fast aromatic ring dynamics.

In summary, we have demonstrated a strategy to produce perdeuterated proteins with isolated <sup>1</sup>H-<sup>13</sup>C pairs in the aromatic ring systems. It is shown that the aromatic side chains of calmodulin have a wide range of motion on the sub-nanosecond time scale, the observation of which has thus far been restricted to detection at natural abundance using highly concentrated and relatively small proteins.<sup>37</sup> The ability to investigate the fast

dynamics of aromatic side chain will provide a highly complementary perspective to that accessed by  $^{13}\text{C}$  or  $^2\text{H}$  relaxation in methyl groups.

## Supplementary Material

Refer to Web version on PubMed Central for supplementary material.

## Acknowledgments

This work was supported by NIH grant GM 102447.

## REFERENCES

1. Mittermaier A, Kay LE. *Science*. 2006; 312:224–228. [PubMed: 16614210]
2. Jarymowycz VA, Stone MJ. *Chem. Rev.* 2006; 106:1624–1671. [PubMed: 16683748]
3. Igumenova TI, Frederick KK, Wand AJ. *Chem. Rev.* 2006; 106:1672–1699. [PubMed: 16683749]
4. Marlow MS, Dogan J, Frederick KK, Valentine KG, Wand AJ. *Nat. Chem. Biol.* 2010; 6:352–358. [PubMed: 20383153]
5. Lee AL, Urbauer JL, Wand AJ. *J. Biomol. NMR.* 1997; 9:437–440. [PubMed: 9255947]
6. LeMaster DM. *Prog. NMR Spectr.* 1994; 26:371–419.
7. LeMaster DM, Kushlan DM. *J. Am. Chem. Soc.* 1996; 118:9255–9264.
8. Wand AJ, Bieber RJ, Urbauer JL, McEvoy RP, Gan ZH. *J. Magn. Res. Ser. B.* 1995; 108:173–175.
9. Ishima R, Petkova AP, Louis JM, Torchia DA. *J. Am. Chem. Soc.* 2001; 123:6164–6171. [PubMed: 11414851]
10. Tugarinov V, Kay LE. *Biochemistry.* 2005; 44:15970–15977. [PubMed: 16331956]
11. Kainosho M, Guntert PQ. *Rev. Biophys.* 2009; 42:247–300.
12. Thomas KA, Smith GM, Thomas TB, Feldmann RJ. *Proc. Nat. Acad. Sci. USA.* 1982; 79:4843–4847. [PubMed: 6956896]
13. Burley SK, Petsko GA. *Science.* 1985; 229:23–28. [PubMed: 3892686]
14. Burley SK, Petsko GA. *FEBS Lett.* 1986; 203:139–143. [PubMed: 3089835]
15. Dill KA. *Biochemistry.* 1990; 29:7133–7155. [PubMed: 2207096]
16. Birtalan S, Fisher RD, Sidhu SS. *Mol. Biosystems.* 2010; 6:1186–1194.
17. Bogan AA, Thorn KS. *J. Mol. Biol.* 1998; 280:1–9. [PubMed: 9653027]
18. Bartlett GJ, Porter CT, Borkakoti N, Thornton JM. *J. Mol. Biol.* 2002; 324:105–121. [PubMed: 12421562]
19. Wüthrich K, Wagner G. *FEBS Lett.* 1975; 50:265–268. [PubMed: 234403]
20. Boyer JA, Lee AL. *Biochemistry.* 2008; 47:4876–4886. [PubMed: 18393447]
21. Teilum K, Brath U, Lundstrom P, Akke M. *J. Am. Chem. Soc.* 2006; 128:2506–2507. [PubMed: 16492013]
22. Lundstrom P, Teilum K, Carstensen T, Bezsonova I, Wiesner S, Hansen DF, Religa TL, Akke M, Kay LE. *J. Biomol. NMR.* 2007; 38:199–212. [PubMed: 17554498]
23. Lee AL, Flynn PF, Wand AJ. *J. Am. Chem. Soc.* 1999; 121:2891–2902.
24. Berg, JM.; Tymoczko, JL.; Stryer, L. *Biochemistry*. 6th ed.. W.H. Freeman; New York: 2007.
25. Kranz JK, Flynn PF, Fuentes EJ, Wand AJ. *Biochemistry.* 2002; 41:2599–2608. [PubMed: 11851407]
26. Liu WX, Flynn PF, Fuentes EJ, Kranz JK, McCormick M, Wand AJ. *Biochemistry.* 2001; 40:14744–14753. [PubMed: 11732893]
27. Kalan EB, Davis BD, Srinivasan PR, Sprinson DB. *J. Biol. Chem.* 1956; 223:907–912. [PubMed: 13385238]
28. Srinivasan PR, Shigeura HT, Sprecher M, Sprinson DB, Davis BD. *J. Biol. Chem.* 1956; 220:477–497. [PubMed: 13319365]
29. Tjandra N, Feller SE, Pastor RW, Bax A. *J. Am. Chem. Soc.* 1995; 117:12562–12566.

30. Kuboniwa H, Tjandra N, Grzesiek S, Ren H, Klee CB, Bax A. *Nat. Struct. Biol.* 1995; 2:768–776. [PubMed: 7552748]
31. Lipari G, Szabo A. *J. Am. Chem. Soc.* 1982; 104:4546–4559.
32. Ye CH, Fu RQ, Hu JZ, Hou L, Ding SW. *Magn. Reson. Chem.* 1993; 31:699–704.
33. Ottiger M, Bax A. *J. Am. Chem. Soc.* 1998; 120:12334–12341.
34. Yao LS, Grishaev A, Cornilescu G, Bax A. *J. Am. Chem. Soc.* 2010; 132:4295–4309. [PubMed: 20199098]
35. Dellwo MJ, Wand AJ. *J. Am. Chem. Soc.* 1989; 111:4571–4578.
36. Goldman M. J. *Magn. Reson.* 1984; 60:437–452.
37. Palmer AG, Hochstrasser RA, Millar DP, Rance M, Wright PE. *J. Am. Chem. Soc.* 1993; 115:6333–6345.

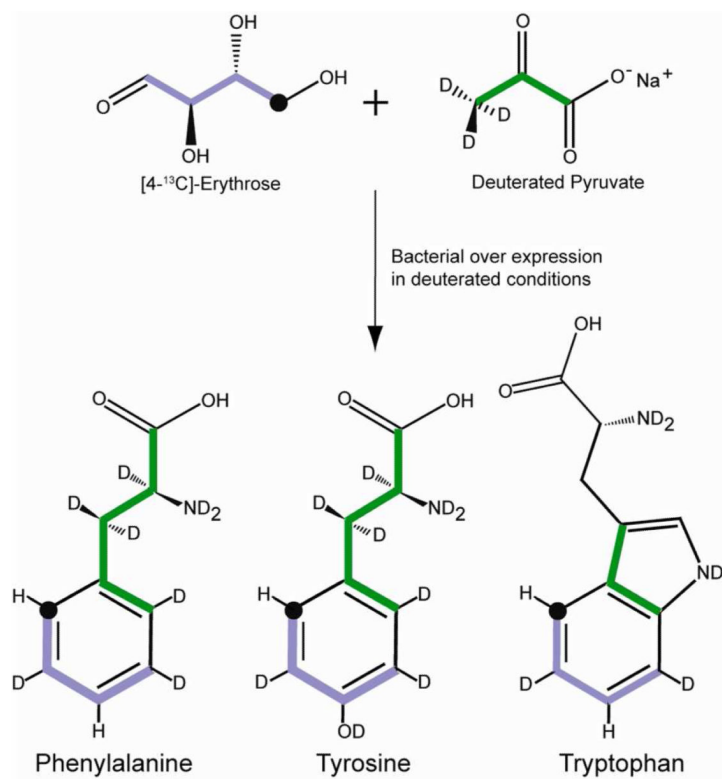


**Figure 1.** Carbon inflow into the aromatic pathway through the condensation reaction of erythrose 4-phosphate and phosphoenolpyruvate. Green and purple highlighting indicates the carbon originating from pyruvate and erythrose, respectively. The position of the <sup>13</sup>C label is indicated by ‘•’.

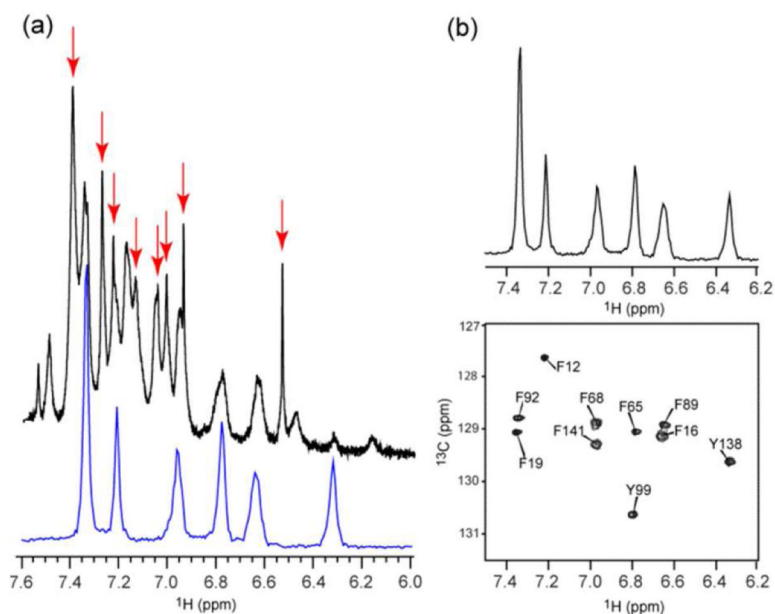


**Figure 2.**

(a) Overlay of the one-dimensional  $^1\text{H}$  spectrum of aromatic region from  $^{13}\text{C}$  filtered and decoupled (lower, blue) and unfiltered  $^1\text{H}$  spectrum (upper, black) of calcium-saturated calmodulin expressed during growth on  $[4\text{-}^{13}\text{C}]$ -erythrose, deuterated pyruvate and  $\text{D}_2\text{O}$  indicating a selective introduction of a  $^1\text{H}$ - $^{13}\text{C}$  pair at a single  $\delta$ -carbon of Phe and Tyr. Also evident are resonances arising from hydrogen bonded to  $^{12}\text{C}$  at the  $\zeta$  position of the aromatic ring of Phe (red arrows). These resonances have narrow line widths due to the absence of scalar coupling. A more detailed analysis of the  $^1\text{H}$  spectrum is presented in the supplementary (Fig. S1 and S2). (b) The two-dimensional  $^{13}\text{C}$ -HSQC spectrum of the aromatic region and the corresponding one-dimensional  $^1\text{H}$  spectrum ( $^{13}\text{C}$  filtered) are shown. No significant  $^{13}\text{C}$  labeling of other amino acids was observed.

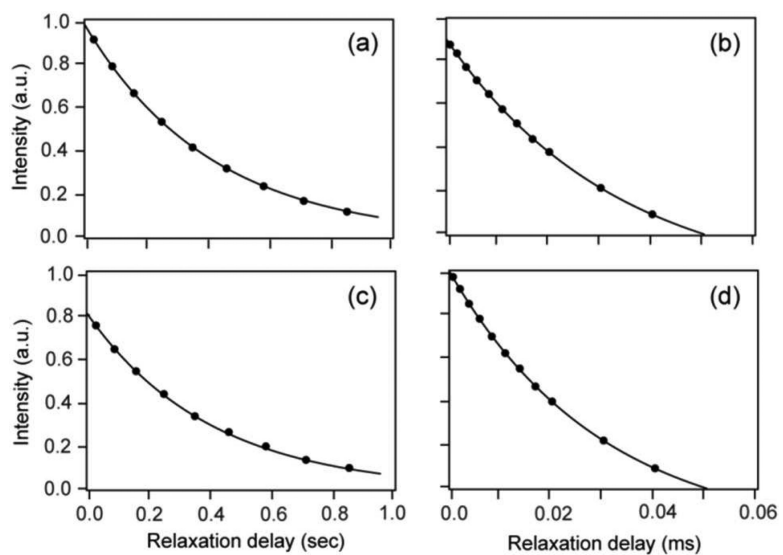


**Figure 3.** Aromatic  $^{13}\text{C}$  R1 and R1 $\rho$  relaxation in calcium-saturated calmodulin prepared using [4- $^{13}\text{C}$ ]-erythrose/deuterated pyruvate/D $_2\text{O}$  strategy (Panels a and b) or a [1- $^{13}\text{C}$ ]-glucose strategy (Panels c and d). Relaxation at the delta-2 position of F92 is shown.



Table 1

Lipari-Szabo model-free parameters for aromatic ring motion in calcium-saturated calmodulin<sup>a</sup>

Probe	$O^2$	$\tau_e$ (ps)	Probe	$O^2$	$\tau_e$ (ps)
F12 <sup>b</sup>	0.49 ± 0.03	236 ± 21	F89 <sup>c</sup>	0.94 ± 0.02	900 ± 39
F16 <sup>b,d</sup>	0.95 ± 0.01	127 ± 12	F92 <sup>c</sup>	0.72 ± 0.03	624 ± 23
F19 <sup>b</sup>	0.47 ± 0.01	232 ± 19	Y99 <sup>c</sup>	0.79 ± 0.02	240 ± 21
F65 <sup>b</sup>	0.70 ± 0.04	176 ± 23	Y138 <sup>c</sup>	0.89 ± 0.02	604 ± 36
F68 <sup>b</sup>	0.96 ± 0.01	292 ± 17	F141 <sup>c</sup>	0.95 ± 0.01	101 ± 11

<sup>a</sup>Prepared using the [4-<sup>13</sup>C]-erythrose labeling scheme. Model-free squared generalized order parameters ( $O^2$ ) and effective correlation times ( $\tau_e$ ) determined using the simple model-free spectral density,<sup>31</sup> an effective C-H bond length of 1.09 Å, and the axially symmetric and fully anisotropic chemical shift anisotropy tensors for the  $\delta$ -<sup>13</sup>C of Phe and Tyr, respectively, as determined by Ye et al.<sup>32</sup> Macromolecular tumbling was characterized using <sup>15</sup>N-relaxation with an effective N-H bond length<sup>33</sup> of 1.04 Å and a simple uniform <sup>15</sup>N chemical shift anisotropy tensor breadth<sup>34</sup> of -170 p.p.m. The N- and C-terminal domains were treated separately. The precision of the squared generalized order parameters ( $O^2$ ) and effective correlation times ( $\tau_e$ ) were estimated by Monte Carlo sampling.

<sup>b</sup>Part of the N-terminal domain with an effective macromolecular tumbling time of 8.96 ± 0.14 ns.

<sup>c</sup>Part of the C-terminal domain with an effective macromolecular tumbling time of 8.05 ± 0.10 ns.

<sup>d</sup>Due to partial spectral overlap, only data obtained at 17.6 T was fitted.